Theoretical Analysis of the Transmission Efficiency of a (6 + 1) × 1 Pump–Signal Combiner

Lucas Salustiano Mendes
University of São Paulo
São Paulo, Brazil
orcid.org/0000-0001-8068-1149

Ricardo Elgul Samad
Laser center and applications
IPEN-CNEN/SP
São Paulo, Brazil
orcid.org/0000-0001-7762-8961

Cláudio Costa Motta
University of São Paulo
São Paulo, Brazil
orcid.org/0000-0002-2508-7320

2022 SBFoton International Optics and Photonics Conference (SBFoton IOPC) | 978-1-6654-5273-1/22/$31.00 ©2022 IEEE | DOI: 10.1109/SBFotonIOPC54450.2022.9992582

***Abstract*—An analytical formulation for the transmission efficiency of a $(6+1)\times1$ pump-signal combiner has been developed and is reported in this paper. The formulation is supported by the Coupled Mode Theory (CMT), and the Finite Difference Beam Propagation Method (FD-BPM). In this scope, the characteristics of commercial fibers FG200AEA, GDF20/200, P-20/400DC are considered to build a combiner computational model. Thus, the CMT was used to estimate the adiabatic length of the input bundle fibers and the combiner efficiency was analyzed based on FD-BPM.**

***Index Terms*—pump-signal combiner, optical fiber taper, coupled-mode theory, Beam Propagation Method, transmission efficiency**

I. Introduction

High-power all-fiber lasers operating in the near and mid-infrared spectral regions are widely used in the free-space communications, light detection and ranging (LiDAR) systems, range finding, remote sensing, and micromachining. Their attractive properties, including excellent beam quality at high output powers, compactness, high transmission efficiency, and low maintenance have facilitated its extensive applications in industry, medicine, research and other areas [1]. In this configuration every optics components, (such as mirrors, and beam combiners) are fiber-made, what enable the light remains in the waveguide up to the laser output, reducing losses, maintaining the beam optical quality and improving the transmission efficiency.

The growing demand for high power fiber lasers has motivated many research groups to develop beam combiners capable of achieve this need. Usually beam combiners are designed in an end-pumping scheme where the input fibers bundle are tapered, fused, and spliced into the output fiber (tapered fiber bundle method-TFB) [2]. This scheme produces devices with high efficiency and reliability which can be employed in $N\times1$, and $(N+1)\times1$ configurations, where N is the pumping fibers number. In 2017 Liu *et al* [3] published the results of building a pump and signal end-pumped combiner where the output fiber underwent a tapering process to minimize mismatches between the signal and output fibers reaching an efficiency of 87.52% signal power transmission and 98.56% for pump power transmission. Also in 2017 Zou *et al* [4] published the results of building a pump and signal combiner with signal and pump power transmission efficiency of 97.7% and 98% respectively. In that work, the pump fibers were tapered keeping a gap for the signal fiber. After the tapering, the signal fiber was inserted and spliced to the output fiber.

In this paper a theoretical approach based on the CMT, and FD-BPM was used to design a $(6+1)\times1$ pump-signal end-pumped combiner. Thus, the fiber bundle (tapers) adiabaticity and efficiency are estimated as a function of length with the aid of CMT. From the CMT results about the bundle length the optical device is build and the optical beam behavior along the device is analyzed with FD-BPM. This last analyse can estimate the pump, and signal transmission efficiency to the beam combiner designed.

II. Theoretical Analysis

The model considers a $(6+1)\times1$ pump-signal combiner which has a signal fiber in the middle of six pump fibers around it. These fibers compose the input fiber bundle with are fused, tapered down, cleaved, and spliced to the output double-clad fiber (DCF), as can seen in Fig.1. The input fibers are inserted in an capillary tube with D_{cap} diameter, and then undergo the tapering process. So, the initial fiber bundle diameter is D_{in}, and after tapering it becomes D_{taper}, which is matched with DCF diameter D_{out}.

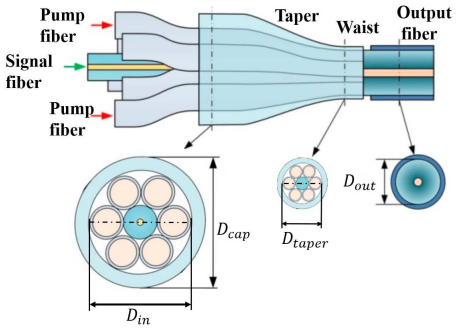

Fig. 1. $(6+1)\times1$ pump-signal combiner, [2].

The power launching efficiency is one of the main features of beam combiner, and its main sources of losses are the losses

978-1- 6654-5273-1/22/$31.00 ©2022 IEEE

due to field propagating in the irregular waveguide (bundle fibers), and the fibers mismatching due to property difference at the interface between bundle fibers and output DCF [5]. So, to achieve a high signal and pump power transmission efficiency, the device tapered fibers must be adiabatic, avoiding the light leakage from the cores. Besides, fiber characteristics must be correctly choose to minimize the mismatch losses.

Thus, consider an beam combiner in which each input fiber has circular symmetry and in the a taper region the core radius, $r = a(z)$, gradually decreasing from a_1 to a_2. Assuming that the taper has a slow decrease with distance, and the fiber radius variation is small compared to the taper extension L, it is possible to describe the taper shape as a z-function [6]. In the case of multi-mode signal fibers, they obey the basic rule that a taper should be characterized by a gradual and slow core diameter decrease, known as the adiabatic criterion for tapering, which can be written as [7]:

$$\frac{dr}{dz} \leq \frac{a(z)}{Z_p}, \tag{1}$$

where dr/dz describes the radius rate of change with the taper coordinate, $Z_p = 2r/NA$ is the half period between reflections, and NA is the fiber numerical aperture. Using Eq.(1) it is possible to calculate the minimum taper length fulfilling the adiabatic criterion:

$$L_{min} \geq \frac{2(a_1 - a_2)}{NA}. \tag{2}$$

Additionally, to avoid significant losses, the beam brightness is proportional to the transmitted optical power and should be preserved. The brightness ratio BR parameter allows us to estimate the transmission loss of the combiner, which can be designated as [2]:

$$BR \approx \frac{D_{out}^2.NA_{out}^2}{M.D_{in}^2.NA_{in}^2} \geq 1, \tag{3}$$

where M, NA_{in}, and NA_{out} are the pump fibers number, the pump, and output fibers numerical apertures, respectively. When $BR \geq 1$ the brightness is maintained and there is no power loss at the input/output fiber interface.

These criteria aid understanding the efficiency physical concepts to fiber taper. However to photonic device development they are not design tools. Thus, CMT and FD-BPM were used to the beam combiner development.

A. Coupled Mode Theory

According to Marcuse [6], the guided modes of a step-index fiber under weakly guiding condition have a predominant transverse field component. This observation allows us to treat the guided mode field ψ as a scalar quantity that does not need to be described by the full set of Maxwell's equations, but can be treated as the solution of the scalar wave equation,

$$\frac{\partial^2\psi}{\partial r^2} + \frac{1}{r}\frac{\partial\psi}{\partial r} + \frac{\partial^2\psi}{\partial z^2} + n^2(r,z)k^2\psi = 0, \tag{4}$$

where $n(r,z)$ is an arbitrary refractive index, k is the plane wave wavenumber, defined by $k = 2\pi/\lambda$, and λ is the wavelength in vacuum. The behavior of the field at any point inside the fiber, in particular in the taper, can be described by the CMT, where the fields can be represented as a superposition of the normal local modes ϕ_ν, and expansion coefficients c_ν, with z-dependent propagation constants $\beta_\nu(z)$:

$$\psi = \sum_{\nu=0}^{\infty} c_\nu(z)\phi_\nu exp\left[-j\int_0^z \beta_\nu\left(z'\right)dz'\right]. \tag{5}$$

Inside the taper, all modes are coupled together so the expansion coefficients, c_ν, are dependent of each other. The expansion coefficients obey the coupled wave equations, so [6]:

$$\frac{dc_\nu}{dz} = \sum_\mu R_{\nu\mu}^{(a)}\ exp\left[j\int_0^z (\beta_\nu - \beta_\mu)dz'\right], \tag{6}$$

where $R_{\nu\mu}^{(a)}$ is the modal coupling coefficient at the boundary between core and cladding, and it is possible to be described the modal coupling coefficient as [6]:

$$R_{\nu\mu}^{(a)} = \frac{2\pi k(n_1 - n_2)}{\beta_\nu - \beta_\mu} a_{(z)} \frac{\partial a_{(z)}}{\partial z} \left[\phi_\nu\phi_\mu\right]_{r=a(z)}, \tag{7}$$

where $a(z)$ is z-dependent core radius, n_1, and n_2 are the core and cladding refractive index, respectively. Considering fibers with large core radius, $R_{\nu\mu}^{(a)}$ can be described as [6]:

$$R_{\nu\mu}^{(a)} = \frac{2u_\nu u_\mu}{u_\mu^2 - u_\nu^2}\frac{1}{a(z)}\frac{\partial a(z)}{\partial z}, \tag{8}$$

where u_ν and u_μ are the core modal radial propagation constants. According to Marcuse, [6], the modal expansion coefficients c_ν represent a measure of the power carried by each mode. So, the normalized output power along the taper or efficiency can be estimated using the equation:

$$\overline{P} = \sum_\nu \left|c_\nu\right|^2. \tag{9}$$

B. Optical beam behavior

The beam behavior along device is great important to beam combiners design, and the FD-BPM is a powerful analysis tool which use the paraxial approximating the exact wave equation to solve it numerically [8]. So, considering Eq.(4) in Cartesian coordinates, using some algebraic manipulations and considering the paraxial approximation, we obtain the equation [8]:

$$(2j\beta)\frac{\partial\psi}{\partial z} = \nabla_\perp^2\psi + \left[n^2(x,y,z)k^2 - \beta^2\right]\psi. \tag{10}$$

The axial constant can be expressed as $\beta = \overline{n}k$, where $\overline{n}$ is the guide effective refractive index. Thus, considering central differences method to discretization Eq.(10), one can obtain an expression to transversal field distribution at axial future point as the weighted sum of the transversal field distribuition at previous and present axial point, as:

$$\psi_{l,m}^{n+1} = \psi_{l,m}^{n-1} - A.D\left(\psi\right)_{l,m}^n + B_{l,m}^n.\psi_{l,m}^n, \tag{11}$$

where l, m, and n are the Cartesian discrete position relative to respective x,y, and z axis respectively. The terms A, $D\left(\psi\right)_{l,m}^{n}$, and $B_{l,m}^{n}$ are the free space propagation coefficient, second order difference, and the waveguide propagation coefficient respectively, and they can be expressed as:

$$A = j\left(\Delta z/\overline{n}k\Delta x^2\right) = j\left(\Delta z/\overline{n}k\Delta y^2\right), \quad (12)$$

$$D\left(\psi\right)_{l,m}^{n} = \psi_{l-1,m}^{n} + \psi_{l+1,m}^{n} + \psi_{l,m-1}^{n} + \psi_{l,m+1}^{n}, \quad (13)$$

$$B_{l,m}^{n} = 2A - j\left(\Delta z k/\overline{n}\right).\left[\left(n_{l,m}^{n}\right)^2 - \overline{n}^2\right]. \quad (14)$$

The waveguide propagation coefficient $B_{l,m}^{n}$ contains information about the device refractive index. Thus, for Eq.(11) to be implemented, it is necessary to build a three-dimensional matrix with device refractive indices spatial distribution. The implementation this matrix is a key point for the analysis in FD-BPM.

The FD-BPM is a powerful tool to analyse the field behavior along device, output power measuring, insertion losses, and transmission efficiency. This tool produces a frame of the transverse distribution of the field at each position along the axial axis. So, integrating the transversal field distributions at the device output and input position, one can obtain its transmission efficiency, as can see in Eq.(15):

$$\eta = \left(\frac{\int\int n_{out}\left(x,y\right).\left|\psi_{out}\left(x,y\right)\right|^2 dxdy}{\int\int n_{in}\left(x,y\right).\left|\psi_{in}\left(x,y\right)\right|^2 dxdy}\right) \times 100\%, \quad (15)$$

where $n_{out}\left(x,y\right)$, $\psi_{out}\left(x,y\right)$,$n_{in}\left(x,y\right)$, and $\psi_{in}\left(x,y\right)$ are the refractive index and transversal field distributions at output and input, respectively.

III. Results and Discussion

The $\left(6+1\right)\times 1$ beam combiner computational implementation is based on technical characteristics provided in components data sheets, as can be observed in Table I. To bundle building was assumed that the input bundle fibers were linearly tapered, fused together, spliced to DCF, and its final diameter matches the output fiber diameter. Thus, the first step is the input fiber bundle analysis.

TABLE I
Material Characteristics

Component	Commercial code	$D_{core}/D_{clad}(\mu m)$	NA
Capillary tube	FTB01	1200/1450	-
Pumping fiber	FG200	200/220	0.22
Signal fiber	GDF	20/200	0.06
Output DCF	P-20/400DC	20/400	0.06/0.46

Analysing firstly the pump fibers, they allow the guidance of thousands of modes, but in a similar way to the works of Hang Zhou [10], and Yang Cao [11], in this work only few modes were analyzed and the normalized power carried by them was considered as the total power in the fiber [9]. In references [10], [11] six modes were analyzed, and in this work two low order modes were analyzed, $LP_{0,1}$, $LP_{1,1}$, together with other eight high-order ones, $LP_{4,5}$, $LP_{1,7}$, $LP_{0,8}$, $LP_{6,8}$, $LP_{3,10}$, $LP_{10,10}$, $LP_{1,15}$ and $LP_{5,15}$. Thus totaling ten modes that are distributed over a wide range of the radial propagation constants allowed by the fiber. For the signal fiber only main mode $LP_{0,1}$, and $LP_{1,1}$ modes can propagate. Thus, its modal analysis was restrict to this modes.

The power flow in each pump fiber was considered to be the same, and the mentioned modes were used to taper power transmission efficiency estimation. So, similarly to the implementation presented in [9], a MATLAB code based on CMT was implemented to calculate the efficiency as a function of the taper length, and the flowchart algorithm can be seen in Fig.2. The modal coupling coefficients and phase constants where stored in a 10×10 triangular matrix, and the simulations were carried out for taper lengths L from $1mm$ to $L_{max} = 20mm$, in $1mm$ steps. Eq.(6) integration is run within secondary loop in steps from $\nu = 1\mu m$ to taper length L. Thus, the algorithm presents the power transmission efficiency for each taper length L. The results for the pump and signal fibers can be seen in Fig.3. In these graphics one can observe what the signal fiber is adiabatic for any taper length bigger than $1mm$. For the pump fiber the efficiency grows rapidly with the taper length increase, presenting an asymptotic behavior for the length from $10mm$ onwards.

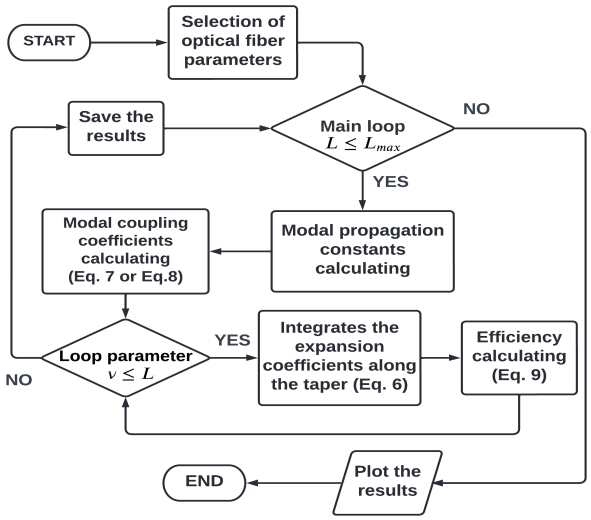

Fig. 2. CMT implementation algorithm Flowchart.

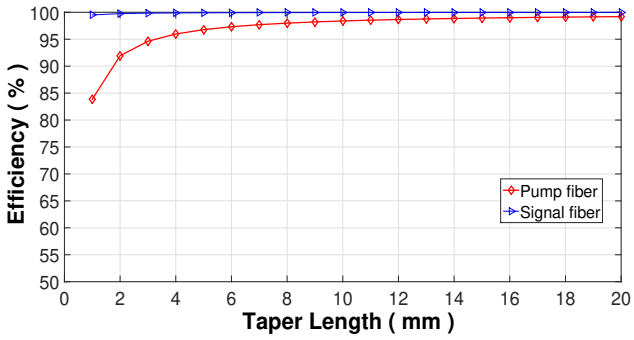

Fig. 3. Signal and pump power transmission efficiency along the taper length.

The second step, one must use Eqs.(11)-(14) in the FD-BPM to analyze the propagation of Gaussian pulses along the device. So the refractive indices three-dimensional matrix must be build to device based on Table I data. In this implementation was considered the core refractive indexes for the DCF and signal fiber, $n_1 = 1.457$, and the others refractive indices were calculated based on relation $n_2 = \sqrt{(n_1^2 - NA^2)}$. To implement the simulation, the taper bundle length was chosen based on results presented in Fig.3. One can observe that, for the pump fibers, taper lengths from $10mm$ onward to $20mm$ present very close efficiency near 100%. Thus, the minimum taper length was choose to the pump taper length, and its used to signal fiber too. Additionally it was used in computational implementation a transition region or waist with $5mm$ and $10mm$ for the output fiber. Fig.4 presents the distributions for the refractive indices in the bundle inlet and in the DCF used in FD-BPM algoritm. To facilitate the operations performed by the software, powers of two (2^N) were used for the dimensions of all matrices. In this way, the transverse grids were discretized with 2^{10} points for each axis and the axial grid with 2^{16} points.

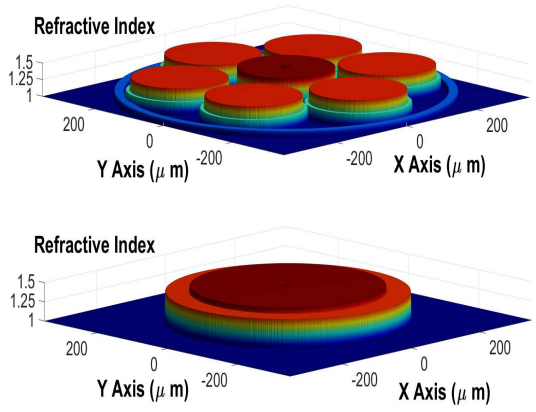

Fig. 4. Bundle and DCF refractive index profile.

Fig.5 presents the flowchart FD-BPM algorithm implemented in this analysis. The code was implemented in Matlab and was used boundary conditions to tangential electric fields, which are continuous at interface region, and transverse electric fields, which are discontinuous in this regions, in accordance with electromagnetic theory [8]. These boundary conditons were implemented in each fiber boundary region. To facilitate the results observation, the simulations with signal and pump lasers were performed separately. The inputs were implemented using Gaussian distribution in Cartesian plane and wavelengths $1064nm$ and $976nm$ to signal and pump lasers, respectively.

The FD-BPM algorithm presents a tranverse field frames sequence to each axial position. However, to analyze the behavior of the field along the device, a cut was performed in the X-Z plane where the behavior of the field propagated from the input to the output of the device can be observed. In Fig.6 one can see that signal field started to propagate with two modes and as the fiber tapers, the propagation becomes single-mode until reaching the output fiber at $15mm$ where the signal returns to propagate with two modes. The figure color bar shows that the beam remains in the same amplitude range, however to measure device signal transmission efficiency Eq.(15) was used, resulting in a 89.01% transmission efficiency.

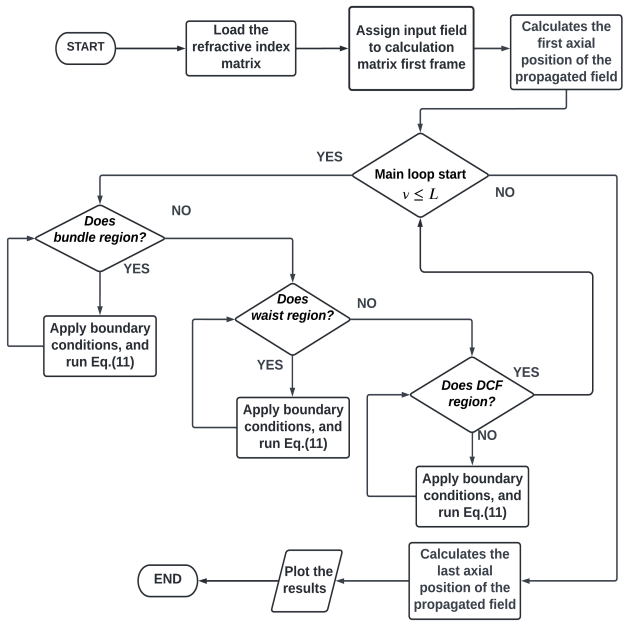

Fig. 5. FD-BPM implementation algorithm Flowchart.

The same method was used for the pump fibers. However, assuming tapers adiabaticity and their geometric distribution showed in Fig.4, one can consider that the field propagating in a given tape does not interfere in the other. So, the propagation was analysed at X-Z device plane and presented in Fig.7, where one can be seen a multimode beam propagating from the input fibers up to output fiber. In this fiber, part of the field propagates in the core as the field reaches it. So, Eq.(15) was used to estimate the pump transmission efficiency resulting a 96.97%.

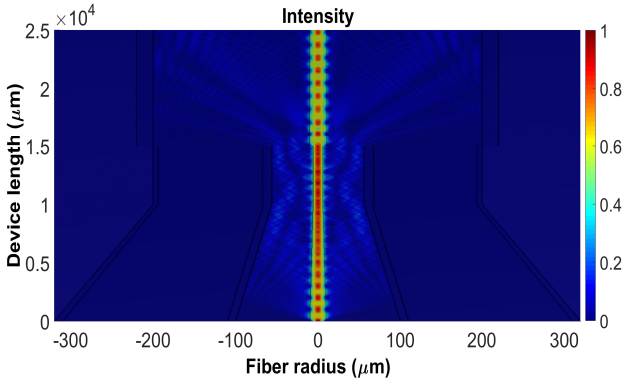

Fig. 6. Propagated signal field along of device.

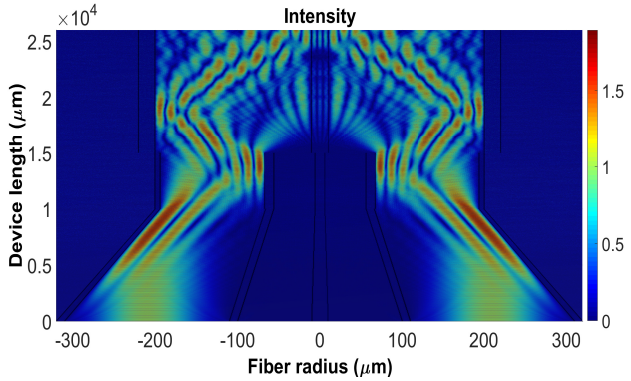

Fig. 7. Propagated pump fields along of device.

Collecting the first and last field samples, it is possible to visualize the electric fields of the pump and signal lasers at the input and output of the device, as we can see in Fig.(8). In the upper portion of the figure, the electric fields for the pump laser are shown. In this figure one can seen the presence of the pumping lasers in the DCF inner cladding and in its core (central part of the figure), as shown in Fig. 7 for the propagated pump field. In the lower portion, the electric fields for the signal laser in the input and output fibers of the device are shown and one can seen an output signal field with approximately single-mode distribution. But, its amplitude is slightly less than the field amplitude at the device input.

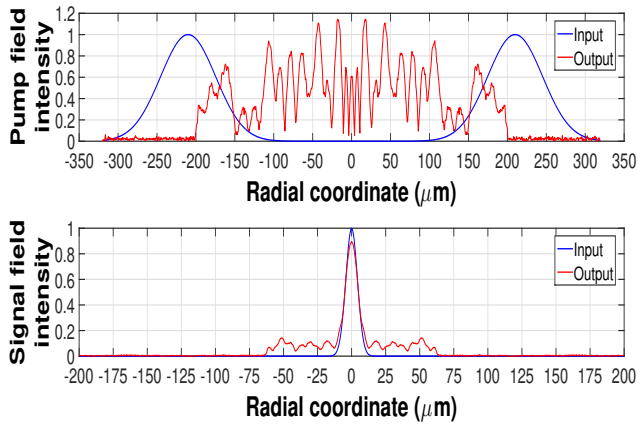

Fig. 8. Pump and Signal field radial distributions.

IV. Conclusion

In this work the theoretical tools CMT and BPM were used to aid in the design of an optical device presenting a theoretical analysis of the power transmission efficiency of a $(6 + 1) \times 1$ pump-signal combiner for step index fibers. The MCT simulations showed that pump and signal fiber tapers with $10mm$ are adiabacitic, producing high efficient fiber tapers. The taper length was used to build the device's refractive index matrix, and run the FD-BPM algorithm to analyze the field behavior and the power transmission efficiency. The algorithms were implemented in Matlab and large matrices were used to represent with accuracy the signal core tapering along the bundle. The results have shown the 89.01% and 96.97% signal and pump transmission efficiency, respectively, which are similar to the results obtained by other research groups [3], [4], [10], and [11].

The pumping power transmission efficiency observed in works published by other research groups is in the range of 96% to 98%. The signal power transmission efficiency ranges from 70% to 96% depending on the design characteristics. The lower power transmission efficiency observed to signal fiber is a consequence of the higher insertion loss for splicing between input and output fibers. In this cenary, the single mode or multimode fibers that allow propagation in few modes only are severely affected by the mismatching between the modal diameters of the optical beams.

Thus, one can be concluded that the results obtained in this work are consistent with the results presented in the literature, and this analysis allows the design of efficient $(6 + 1) \times 1$ pump-signal beam combiners.

References

[1] Zervas, M. N. and Codemard, C. A. High power fiber lasers: a review. IEEE J. Sel. Top. Quantum Electron, v. 20, n. 5, p. 219-241, 2014.

[2] STACHOWIAK, Dorota. High-power passive fiber components for all-fiber lasers and amplifiers application—Design and fabrication. In: Photonics. Multidisciplinary Digital Publishing Institute, 2018. p. 38.

[3] Liu, Kai et al. Low beam quality degradation, high-efficiency pump and signal combiner by built-in mode field adapter. Optica Publishing Group, V. 56, n. 10, 2017, p. 2804–2809.

[4] Zou, Shuzhen et al. High-efficiency $(6 + 1) \times 1$ pump-signal combiner based on low-deformation and high-precision alignment fabrication. Applied Physics, B, V. 123, 2017, p. 288–292.

[5] AZARI, Amin; BANANEJ, Alireza; BELGABAD, Aydin Ashrafi. Theoretical analysis of optimum adiabatic tapering length and pulse shape modulation along tapered multimode fiber. Optik, v. 127, n. 14, p. 5663-5669, 2016.

[6] MARCUSE, Dietrich. Mode conversion in optical fibers with monotonically increasing core radius. Journal of lightwave technology, v. 5, n. 1, p. 125-133, 1987.

[7] A. W. Snyder and J. D. Love, "Optical Waveguide Theory", London, Hall, (1983), Ch 5.

[8] VEETTIKAZHY, Madhu et al. BPM-Matlab: an open-source optical propagation simulation tool in MATLAB. Optics Express, v. 29, n. 8, p. 11819-11832, 2021.

[9] MENDES, Lucas Salustiano et al. Theoretical Analysis of the Efficiency of a 7× 1 End-Pumped Power Combiner. In: 2021 SBMO/IEEE MTT-S International Microwave and Optoelectronics Conference (IMOC). IEEE, 2021. p. 1-3.

[10] Hang Zhou, Zilun Chen, Xuanfeng Zhou, Jing Hou, Jinbao Chen, "All-fiber 7×1 pump combiner for high power fiber laser". Optics Communications, vol 347, pp 137-140, (2015).

[11] Yang Cao, Wei Shi, Quan Sheng, Shijie Fu, Haiwei Zhang, Xiaolei Bai, Liang Qi, Jianquan Yao, "Investigation on high transmission efficiency 7 × 1 pump combiner," Opt. Eng. 55(12), 126102 (2016).